SERVO PERFORMANCE OF A BLDC DRIVE WITH INSTANTANEOUS TORQUE CONTROL

Teck-Seng Low, King-Jet Tseng, Tong-Heng Lee and Kai-Sang Lock
Department of Electrical Engineering
National University of Singapore
10 Kent Ridge Crescent
Singapore 0511

ABSTRACT

Brushless D.C. (BLDC) drives with permanent-magnet motors are suitable as servo motors if properly controlled. Their performance can be superior to conventional D.C. servos if NdFeB or rare-earth cobalt magnets are used for motor excitation and novel control techniques implemented for its servo performance. The availability of inexpensive but high performance digital signal processors, allow the implementation of a novel instantaneous torque control algorithm for BLDC drive applications. This paper presents the servo performances of a BLDC drive with instantaneous torque control. To assess the quality of this controller its performance is compared with those obtained using conventional current controllers. Details of the control strategies are also described.

1. INTRODUCTION

Brushless dc (BLDC) drives using high torque permanent-magnet (PM) motors are suitable for the direct drive applications in servo systems and robots. The advantages of direct drive systems lie in their ability to minimize the friction and backlash associated with geared drives [1-4]. However, the absence of gearing is not without its own problems. Direct drives have to operate at low sppeds, where the effects of torque pulsations become particularly objectionable [5,6]. However, with high performance Digital Signal Processors (DSP's) and fast switching power devices, it is now possible to implement an instantaneous torque controller as the inner loop controller with the outer loop responsible for the eventual speed or position response of the servo system [7,8,9]. This will give a close control of the torque characteristic and hence superior servo performance.

Conventional current controllers aimed to force the stator phase currents to be as close to the reference supplied, usually an ideal sinusoid, as possible for a constant torque command. These are usually synthesized from a hybrid combination of analog and digital devices. However in many cases, the rotor flux distribution may not be exactly sinusoidal, resulting in torque pulsations [10]. The motor also operates under suboptimal conditions. The concept of instantaneous torque control for a BLDC drive is illustrated in Fig. 1. The combination of the 3-phase inverter and the PM motor is regarded as a torque producing unit which accepts a 3-bit digital command from the torque controller. The instantaneous torque feedback signal can be estimated from the knowledge of machine parameters and the measurements of instantaneous currents and rotor position. Thus by designing appropriate control algorithms, it is possible to eliminate torque pulsations by using the direct digital control of the inverter. This would also lead to the optimal operator of the motor in the BLDC drive system and result in improved performance.

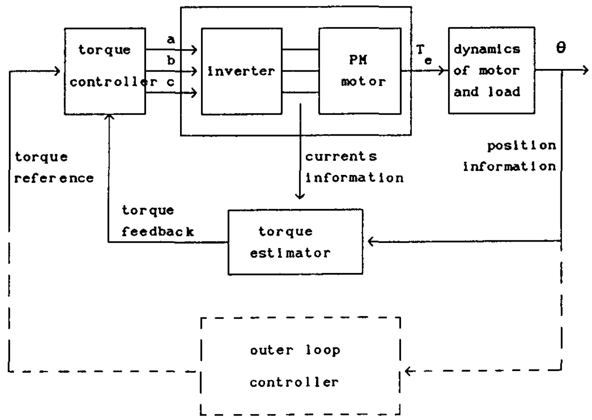

Fig. 1 Concept of instantaneous torque control

This paper describes the performances of a BLDC drive for servo applications using the instantaneous torque control. The applications examined here are speed, position and static torque control. Comparisons are made with respect to those obtained using the conventional current control. Details of their implementations are also given.

2. CONTROL STRATEGIES

2.1 Torque Control [7]

The torque control algorithm is based on the variable structure strategy (VSS) in which the switching signals for the inverter are determined directly by the digital controller. In the VSS system a switching control law is used to drive the plant's state trajectory onto a chosen surface in the state space. This surface is known as the switching surface. In the BLDC drive, the d-q transformation is performed on the motor model so that the states are the direct-axis and quadrature-axis currents, i_d and i_q.

The switching surfaces are selected to be

$$s_d = i_{dref} - i_d \tag{1}$$

$$s_q = T_{ref} - T_e \tag{2}$$

where $i_{dref} = 0$ (for optimal BLDC operation)

90/CH 2935-5/90/0000-0454$01.00©1990 IEEE

T_{ref} = torque reference as determined by the outer loop controller

The VSS control functions are selected to be

$$v_d = V_d \ \mathrm{sgn}(s_d) \tag{3}$$

$$v_q = V_q \ \mathrm{sgn}(s_q) \tag{4}$$

These selections are based on the concept of vector control. The controller determines the control inputs v_d and v_q, which are in the rotating d-q domain, by considering the positions of the state trajectories in the switching plane. There are four possible combinations of v_d and v_q. Their effects can be classified as in Table 1. These control inputs are then mapped into the abc voltage vectors of the inverter. The results of the mapping are shown in Table 2. Figure 2 shows the block diagram of the torque controller.

Table 1: Control Inputs And Actions

Control Inputs	Control Actions
$v_d = +V_d$, $v_q = +V_q$	increase i_d, increase i_q
$v_d = +V_d$, $v_q = -V_q$	increase i_d, decrease i_q
$v_d = -V_d$, $v_q = +V_q$	decrease i_d, increase i_q
$v_d = -V_d$, $v_q = -V_q$	decrease i_d, decrease i_d

Table 2: Mapping To Inverter Vectors

Rotor Angle	Inverter Vectors $v_d=+V_d$ $v_q=+V_q$	$v_d=-V_d$ $v_q=+V_q$	$v_d=-V_d$ $v_q=-V_q$	$v_d=+V_d$ $v_q=-V_q$
345^o- 15^o	1 1 0	0 1 0	0 0 1	1 0 1
15^o- 45^o	1 1 0	0 1 1	0 0 1	1 0 0
45^o- 75^o	0 1 0	0 1 1	1 0 1	1 0 0
75^o-105^o	0 1 0	0 0 1	1 0 1	1 1 0
105^o-135^o	0 1 1	0 0 1	1 0 0	1 1 0
135^o-165^o	0 1 1	1 0 1	1 0 0	0 1 0
165^o-195^o	0 0 1	1 0 1	1 1 0	0 1 0
195^o-225^o	0 0 1	1 0 0	1 1 0	0 1 1
225^o-255^o	1 0 1	1 0 0	0 1 0	0 1 1
255^o-285^o	1 0 1	1 1 0	0 1 0	0 0 1
285^o-315^o	1 0 0	1 1 0	0 1 1	0 0 1
315^o-345^o	1 0 0	0 1 0	0 1 1	1 0 1

2.1.1. *Torque Estimation*

The torque control scheme described in 2.1 requires knowledge of the motor torque. It is not practical to measure the developed motor torque directly by torque transducers such as strain gauges because of the difficulties involved in obtaining a reliable signal without signal processing. Therefore, the torque feedback information is obtained from the knowledge of motor parameters and the measurements of instantaneous currents and rotor position. For a PM motor with non-sunusoidal flux distribution, the torque feedback can be estimated by the following equation,

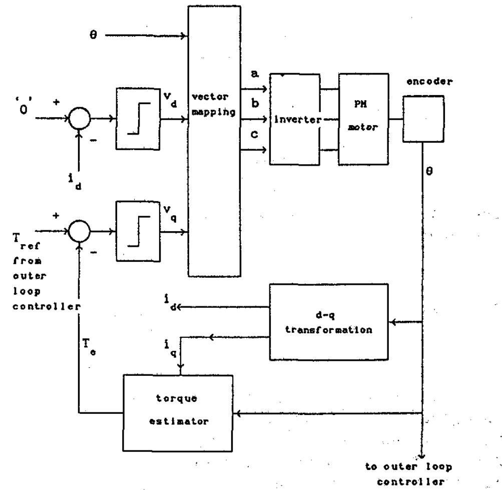

Fig. 2 Block diagram of the torque controller

$$T_e = \frac{3}{2}\frac{P}{2}\left[K_0 + K_6\cos 6\theta + K_{12}\cos 12\theta + \ldots\right] i_q \tag{5}$$

Where P is the no of poles and K_0, K_6, K_{12} ... are functions of the self inductance harmonics in the direct (L_{dfn})and quadrature axis (L_{qfn}), and i_f, the equivalent field excitation current.

$K_0 = L_{dfo}\ i_f$,
$K_6 = (6L_{qf6} + L_{df6})\ i_f$,
$K_{12} = (12L_{qf12} + L_{df12})\ i_f$, ...

To identify the neccessary parameters for the torque calculation the quadrature-axis voltage equation is used as the least squares model equation for the parameter identification process. This torque estimation procedure has been described in an earlier paper [7].

2.2 *Speed Control*

The torque controller for the inner loop can be coupled to a speed controller implemented for the outer loop. To assess the performances of such a system for speed control, a digital PI speed control algorithm is designed and incorporated as the outer loop controller. Figure 3 shows the block diagram of the PI speed controller and the BLDC drive. The inner loop of the BLDC drive is modelled as a zero order hold. The z-transform of the motor and the zero order hold is given by

$$G(z) = \frac{(1 - e^{-aT})}{(z - e^{-aT})} \tag{6}$$

where D = viscosity coefficient of the shaft
J = Moment of inertia
T = Sampling interval
a = D/J

The speed controller employs proportional plus integral action,

$$d(t) = K\,[e(t) + \frac{1}{T_I}\int e(t)\,dt] \tag{7}$$

In z-domain, this PI control action is given by

$$D(z) = (K_p + K_I)\cdot\frac{z - K_p/(K_p + K_I)}{z - 1} \tag{8}$$

where K_p = proportional gain

K_I = integral gain

The open loop transfer function of the system is therefore,

$$D(z)G(z) = (K_p + K_I)\,\frac{(1 - e^{-aT})[z - K_p/(K_p + K_I)]}{(z - 1)(z - e^{-aT})} \tag{9}$$

The desired response of the drive system is obtained by the pole placement method. In this method the desired closed loop poles are located on the z-plane for the desired response from the drive, and by adjustment of the controller parameters (K_p and K_I), the root locus of the drive system can be made to pass through the desired closed loop poles. The values obtained for K_p and K_I then serve as a guide for further tuning.

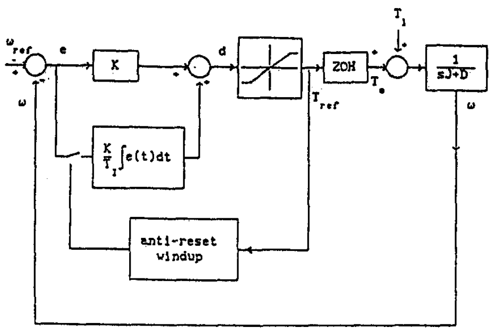

Fig. 3 The PI speed controller

2.3 Position Control

A position control algorithm is implemented as the outer loop controller to test its performance when integrated with the instantaneous torque controller. This control algorithm is based on variable structure strategy. It had been implemented in a BLDC drive system with conventional pwm current control and reported in an earlier publication [12]. To have a well damped response with no overshoot the following switching function is used,

$$s = cx_1 + x_z \tag{10}$$

where x_1 = position error

$x_z = \dot{x}_1$

The VSS control function implemented is,

$$u = \Psi_1 x_1 + \Psi_2 x_2 + k_f \operatorname{sgn}(s) \tag{11}$$

where

$$\Psi_1 = \begin{cases} \alpha_1 & ,\text{if } sx_1 > 0 \\ \beta_1 & ,\text{if } sx_1 < 0 \end{cases}$$

$$\Psi_2 = \begin{cases} \alpha_2 & ,\text{if } sx_2 > 0 \\ \beta_2 & ,\text{if } sx_2 < 0 \end{cases}$$

$$\operatorname{sgn}(s) = \begin{cases} 1 & ,\text{if } s > 0 \\ -1 & ,\text{if } s < 0 \end{cases}$$

The first term in Eq. 11 is like a normal proportional term, the second term is a form of velocity feedback, and the third term is a relay type term which is commonly used in control systems to overcome the effects of backlash and coulomb frictional forces.

The VSS control system in sliding mode must satisfy the existence condition,

$$\lim_{s\to 0} s\dot{s} < 0 \tag{12}$$

A sufficient condition is that the gain constants satisfy the following inequalities,

$$\begin{cases} -(1/J)\alpha_1 < 0 & ,\text{if } sx_1 > 0 \quad \Rightarrow \alpha_1 > 0 \\ -(1/J)\beta_1 > 0 & ,\text{if } sx_1 < 0 \quad \Rightarrow \beta_1 < 0 \end{cases}$$

$$\begin{cases} c - (\alpha_2 + D)/J < 0 & ,\text{if } sx_2 > 0 \quad \Rightarrow \alpha_2 > (cJ - D) \\ c - (\beta_2 + D)/J > 0 & ,\text{if } sx_2 < 0 \quad \Rightarrow \beta_2 < (cJ - D) \end{cases}$$

$$-(k_f/J)\,|s| + s.f(x,t) < 0$$

$$k_f > T_L \operatorname{sgn}(s)$$

Thus $\quad k_f > T_L$

α_1 and β_1 are easily chosen to satisfy the above conditions and are significant when the error is large and negligible when the error is small. The value of α_2 is chosen with maximum inertia while β_2 is chosen with minimum inertia. The value of k_f is selected with maximum load torque T_L.

3. HARDWARE IMPLEMENTATION

The digital control strategies proposed in section 2 have been implemented with a digital signal processor, the DSP32 manufactured by AT&T [13]. This particular device is chosen because the torque control and torque estimation algorithms require very fast computations in order to limit the chatterings of the phase currents. The DSP32 is supported by a microcomputer which serves as a host development system during the development of the control application programs and provides Input/Output facilities during real-time testing of the programs. This allows for speedy program development, debugging and testing. It is also versatile and can be expanded into a multi-motor controller. For a practical commercial design, the DSP can be permanently masked-programmed with the fully tested application programs and provided with its I/O facilities so that it can operate as a stand-alone controller.

4. CONTROLLER PERFORMANCE

4.1 *Speed Control*

Both the sinusoidal current control and the instantaneous torque control are tested with the speed controller. Four sets of tests have been conducted for each control scheme combination. The test conditions are shown in Table 3. The sampling time for the speed controller is chosen to be 1 ms.

Table 3: Test Conditions For Speed Control $K_p = 1.20$, $K_I = 0.05$

Test No.	Test Conditions
1	speed reference = 10 rpm, load = 0.15 Nm
2	speed reference = 10 rpm, load = 0.55 Nm
3	speed reference = 1 rpm, load = 0.15 Nm
4	speed reference = 1 rpm, load = 0.55 Nm

Table 4: Speed Control Performance Indices

Test No.	Sinusoidal Current Control		Instantaneous Torque Control	
	Settling Time(sec)	SRF	Settling Time(sec)	SRF
1	0.35	0.09	0.32	0.03
2	0.25	0.15	0.32	0.06
3	0.21	0.25	0.23	0.10
4	0.17	0.26	0.23	0.11

The time responses of the system for a step speed command are shown in Figs. 4 to 7. The results show that speed ripples are negligible for the combination of PI speed control and instantaneous torque control. Large variations in speed occur for the speed and sinusoidal current control combination, especially at very low speeds. The settling times and Speed Ripple Factors for all the tests are tabulated in Table 4. Settling time is defined as the time taken for the response curve to reach within 5% of the final value. Speed Ripple Factor (SRF) is defined as the ratio of peak-to-peak speed ripple to the mean speed.

$$SRF = \frac{\delta\omega_{pp}}{\omega_{mean}} \tag{13}$$

The settling times for speed control with instantaneous torque control are more consistent in the presence of load variations and the SRFs are always smaller. From the results, it can be seen that instantaneous torque control has improved the transient and steady-state responses of BLDC drive for speed control applications.

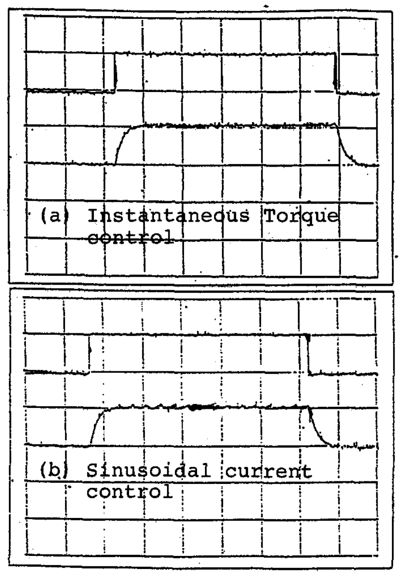

Fig. 4 Experimental results for speed control: Test 1

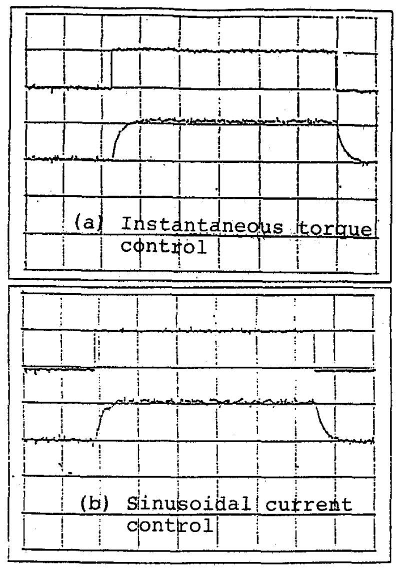

Fig.5 Experimental results for speed control: Test 2

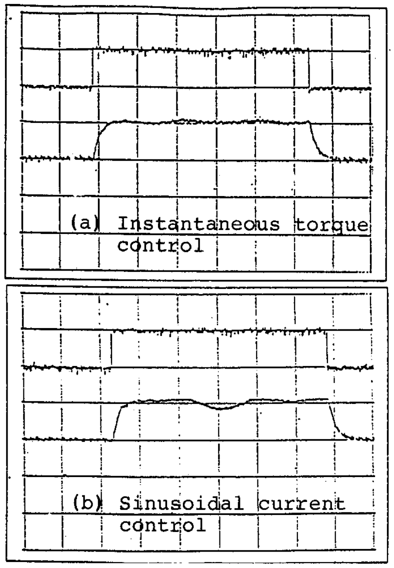

Fig.6 Experimental results for speed control: Test 3

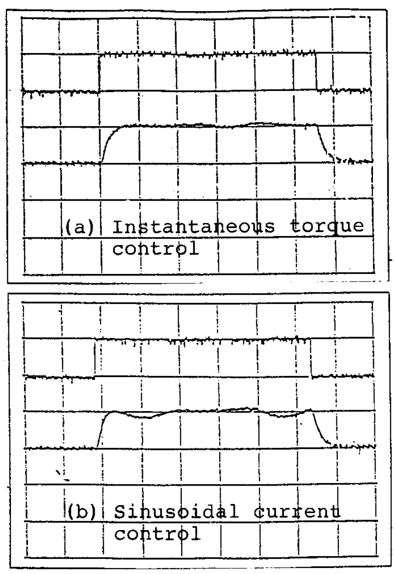

Fig.7 Experimental results for speed control: Test 4

4.2 Position Control

The performance for position control are also obtained using both sinusoidal current control and instantaneous torque control. The results are shown in Figs 8 and 9 for two different loading conditions. In both cases, overshoots are observed for the position curves obtained using sinusoidal current control. The instantaneous torque control scheme exhibits fast but well-damped responses with no overshoot. The incorporation of instantaneous torque control in the inner loop has improved the transient performance of the position controller.

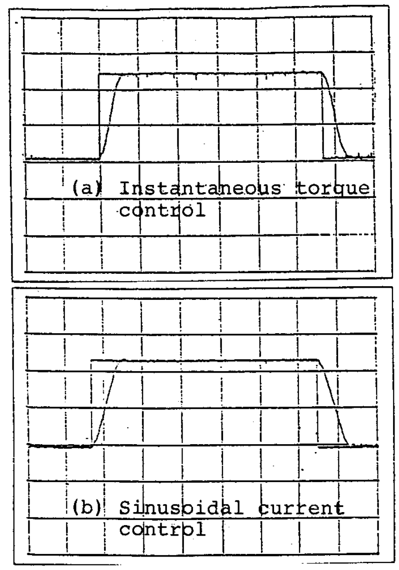

Fig.8 Experimental results for position control (no load)

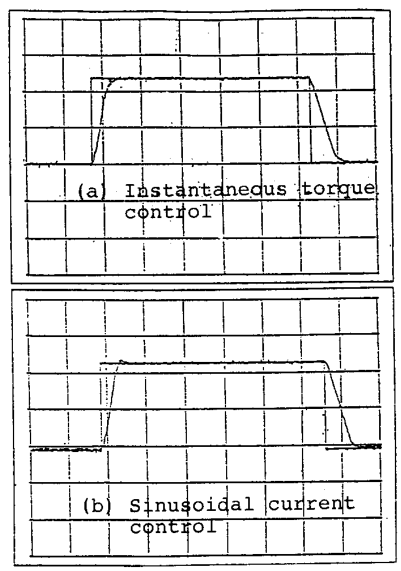

Fig.9 Experimental results for position control (load = 2.0 Nm)

4.3 Static Torque Control

The instantaneous torque control scheme proposed can control the developed torque on the motor shaft even when the shaft is stationary. In this test, the shaft of the rotor is locked in a fixed position. The instantaneous torque control scheme is used to control the static torque for a range of torque references. The developed torque is measured by a torque transducer. The readings are tabulated in Table 4 and plotted in Fig. 10. The results show that the accuracy of the developed static torque is accurate within the working range of the motor to 94%.

Table 5: Static Torque Control
(All figures in Nm)

Torque Reference	Shaft Torque	Absolute Error
0.0	0.0	0.0
0.5	0.47	0.03
1.0	0.95	0.05
1.5	1.47	0.03
2.0	2.02	0.02
2.5	2.56	0.04
3.0	3.06	0.06
3.5	3.58	0.08
4.0	4.07	0.07
4.5	4.58	0.08
5.0	5.05	0.05

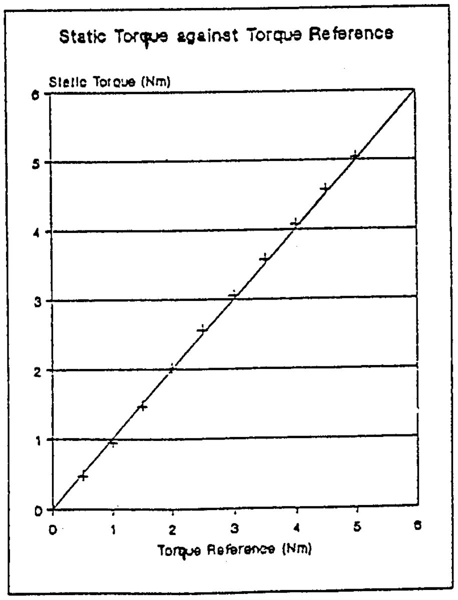

Fig. 10 Accuracy of static torque production

5. CONCLUSIONS

The concept of instantaneous torque control has been introduced for BLDC drive control as an alternative to the conventional sinusoidal current control with the aim of minimization of torque pulsations and optimal useful torque production. The torque control algorithm is based on variable structure strategy. This has been implemented on a DSP-based controller.

The performances of the BLDC drive for servo applications using instantaneous torque control have been examined. In all these applications: speed control, position control and static torque/force control, the results show that the instantaneous torque control has improved the performances when compared to a system with sinusoidal current control. Static torque/force control has also been shown to be accurate.

6. REFERENCES

1. Low T.S., Binns K.J., Rahman M.F., and Wee L.B., "A Nd-Fe-B excited permanent-magnet motor - design and performance," 3rd International conference on Electrical Machines and Drives, IEE, London, Nov 16-18, 1987, pp. 246-249.

2. Low T.S., "Permanent-magnet motors for direct drive applications," Automation News, Nov 1987, pp. 14-17.

3. Asada H., Kanade T., and Takayama I., "Control of a direct drive arm," Trans ASME, Vol. 105, Sep 1983, pp. 136-142.

4. Davies S., and Chen D., "High performance brushless dc motors for direct drive robot arm," PCIM, Aug 1985, pp. 35-38.

5. Hoang L., Perret R., and Feuillet R., "Minimization of torque ripples in brushless dc motor drives," IEEE Transactions on Industry Applications, Vol. 1A-22, No. 4, Jul 1986, pp. 748-755.

6. Ng B.H., Low T.S., Lim K.W., and Rahman M.F., "An investigation into the effects of machine parameters on the torque pulsations in a brushless dc drive," Proc 1988 Conf. Industrial Electronics (IECON '88), Singapore, Oct 24-28, 1988, pp. 749-754.

7. T.S. Low, K.J. Tseng and K.S. Lock, "A strategy for the instantaneous torque control of permanent-magnet brushless D.C. drives", To be published in Proc. IEE Pt. B.

8. Tseng K.J., Low T.S., and Lock K.S., "Torque Control in Permanent-Magnet Brushless DC Drives," Symposium on Motion Control, Singapore, Apr 6, 1989, pp. 12-30.

9. Low T.S., Tseng K.J., Lock K.S., and Lim K.W., "Instantaneous Torque Control," 4th International Conference on Electrical Machines and Drives, London, Sep 13-15, 1989, pp. 100-105.

10. Ng B.H., "An investigation into the effects of machine parameters on the torque pulsations in a brushless dc drive," M.Eng Thesis, 1988, National University of Singapore.

11. Rahman M.F., Low T.S., and Wee L.B., "Development of a digitally controlled brushless dc drive system," Proc. 1986 Conf. Appl. Motion Control (CAMC '86), Minneapolis, Minn., Jun 10-12, 1986, pp. 283-288.

12. Wee L.B., Lim K.W., Low T.S., and Rahman M.F., "A variable structure strategy for motion control," Proc. 1987 Conf. Industrial Electronics (IECON '87), Cambridge, Massachusetts, Nov 3-6, 1987, pp. 167-174.

13. WE DSP32 Digital Signal Processor Information Manual, The AT&T Documentation Management Organization, Sep 1986.